Research Article

Journal of Physical Organic Chemistry

Received: 21 July 2008, Revised: 27 August 2008, Accepted: 27 August 2008, Published online in Wiley InterScience: 22 September 2008

(www.interscience.wiley.com) DOI 10.1002/poc.1452

Ab initio and DFT calculations on the gas phase elimination kinetics of 2,2-diethoxy-ethylamine and 2,2-diethoxy-*N*,*N*-diethyl-ethylamine

José Ramón Mora[a], María Tosta[a], Tania Cordova[b] and Gabriel Chuchani[a]*

The mechanisms for the gas phase molecular elimination kinetics of 2,2-diethoxy-ethylamine and 2,2-diethoxy-*N*,*N*-diethyl-ethylamine were examined at MP2/6-31G, B3LYP/6-31G, B3LYP/6-31G(d,p), MPW91PW91/6-31G. MPW91PW91/6-31G(d,p), PBEPBE/6-31G, and PBEPBE/6-31G(d,p) levels of theory. These elimination processes involve two parallel reactions. The first parallel reaction gives ethanol and the corresponding 2-ethoxyethenamine. The latter compound further decomposes to ethylene, CO, and the corresponding amine. The second parallel reaction produces ethane and the corresponding ethyl ester of an α-amino acid. Calculated thermodynamic and kinetic parameters from PBEPBE calculations were found to be in good agreement with the experimental values. The transition states of the parallel reactions are best described as four-membered cyclic structures. The intermediate 2-ethoxy-ethenamine undergoes a consecutive elimination through a six-membered cyclic transition state mechanism. Bond indexes and synchronicity (Sy) parameters are in agreement with concerted semi-polar transition state structures. Copyright © 2008 John Wiley & Sons, Ltd.

Keywords: 2,2-diethoxy-ethylamine; 2,2-diethoxy-*N*,*N*-diethyl-ethylamine; kinetics; gas phase elimination; parallel reactions; *ab initio* and DFT calculations

INTRODUCTION

Ketals are interesting organic compounds that had little been investigated in gas phase elimination reactions. Among the few reported thermal decomposition of ketals are the works on ethylal, dimethyl acetal, and diethyl acetal, carried out in a static system and over the temperature range of 389–530 °C.[1] A free radical reaction was thought to occur with ethylal, while a rearrangement process was believed to be important in dimethyl and diethyl acetals. In the case of dimethyl acetal, up to 50% decomposition, the reaction was found to follow a first-order rate law as depicted in reaction (1).

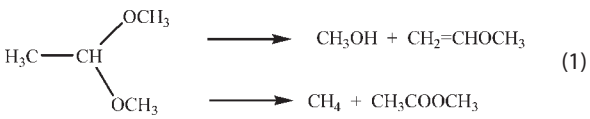

(1)

The pyrolysis kinetics of methylal,[2] ethylene methylal and propylene methylal[3] in the gas phase, was explained in terms of biradical mechanism as described in reaction (2).

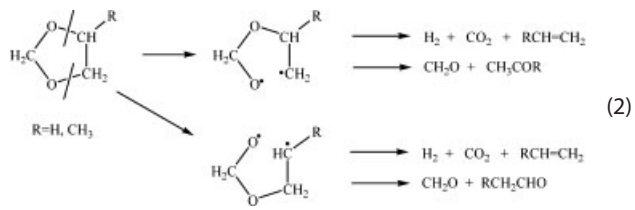

(2)

Molera and Pereira[4,5] revisited the work on the thermal decomposition of methylal in a flow system, but the result was found to be a more complex radical reaction.

A most recent publication in the gas phase elimination kinetics of 2,2-diethoxy-ethylamine and 2,2-diethoxy-*N*,*N*-diethyl-ethanamine[6] was reported to be homogeneous and a unimolecular process. These eliminations, in deactivated reaction vessel, obey a first-order rate law, involving two parallel reactions (3). Step 1 yields ethanol and the corresponding 2-ethoxyethenamine. The latter intermediate further decomposes step 3 to ethylene, CO, and the corresponding amine. The second parallel reaction step 2 gives the corresponding ethyl ester of an *a*-amino acid and ethane gas. According to the results of this work,[6] the experimental kinetic and thermodynamic parameters led to rationalize the mechanisms as described in reaction (3).

* *Correspondence to: G.Chuchani, Centro de Química, Instituto Venezolano de Investigaciones Científicas (I.V.I.C.), Apartado 21827, Caracas, Venezuela. E-mail: chuchani@ivic.ve*

a *J. R. Mora, M. Tosta, G. Chuchani*
Centro de Química, Instituto Venezolano de Investigaciones Científicas (I.V.I.C.), Apartado 21827, Caracas, Venezuela

b *T. Cordova*
Escuela de Química, Facultad de Ciencias, Universidad Central de Venezuela, Apartado 1020-A, Caracas, Venezuela

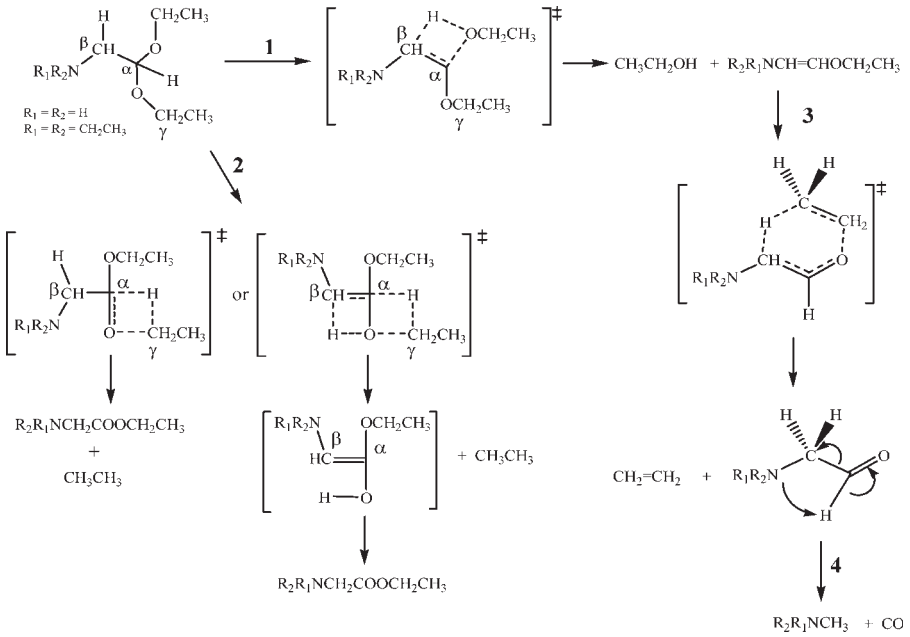

(3)

Since the gas phase elimination kinetics of 2,2-diethoxyethyl amine and 2,2-diethoxy-*N*,*N*-diethylethanamine proved to be homogeneous and unimolecular in nature,[6] the present work aimed at studying these reactions through some theoretical calculations for a reasonable understanding of these mechanisms. Therefore, the present work aimed at studying the potential energy surface (PES) at the *ab initio* and DFT levels of theories.

COMPUTATIONAL METHODS AND MODELS

Ab initio MP2 and DFT model theories were used to investigate the PES and possible intermediate and transition states structures in the gas phase elimination reaction of 2,2-diethoxy-ethylamine and 2,2-diethoxy-*N*,*N*-diethyl-ethylamine. DFT models include functional B3LYP, MPW1PW91, and PBEPBE/6-31G with bases set 6-31G and 6-31G (d,p). Calculations were carried out in Gaussian 03.[7] The Berny standard algorithm was used for analytical gradient optimization routines with convergence on the density matrix was 10^{-9} atomic units, the threshold value for maximum displacement was 0.0018 Å, and that for the maximum force was 0.00045 Hartree/Bohr. Transition states structures were searched using the Quadratic Synchronous Transit protocol. Optimized geometries for reactants, products, and transition states structures at each theory level were characterized by using frequency by means of normal-mode analysis. The unique imaginary frequency associated with the transition vector (TV), that is, the eigenvector associated with the unique negative eigenvalue of the force constant matrix, has been characterized. Intrinsic reaction coordinate (IRC) calculations were performed to further verify transition state structures.[8]

Thermodynamic quantities, such as zero point vibrational energy (ZPVE), temperature corrections ($E(T)$), and absolute entropies ($S(T)$), were obtained from frequency calculations. Rate coefficients were estimated assuming that the transmission coefficient is equal to 1. Temperature corrections and absolute entropies were obtained assuming ideal gas behavior from the harmonic frequencies and moments of inertia by standard methods[9] at average temperature and pressure values within the experimental range. Scaling factors for frequencies and zero point energies for the methods used are taken from the literature.[10] For PBEPBE and MPW91PW91 corrections, B3LYP values were used.

Method	f_{VIB}	f_{ZPE}
B3LYP/6-311G(d,p)	0.97	0.99
MPW91PW91/6-31G(d,p)	0.97	0.99
PBEPBE	0.97	0.99
MP2(Full)/6-31G(D)	0.9427	0.9676

Rate coefficients $k(T)$ were estimated using classical TST[11–13] assuming that the transmission coefficient is equal to 1, as expressed in the following expression:

$$k(T) = (k_B T/h)\ \exp(-\Delta G^{\#}/RT)$$

where $\Delta G^{\#}$ is the Gibbs free energy change between the reactant and the transition state and k_B, h are the Boltzmann and Planck constants, respectively.

$\Delta G^{\#}$ was calculated using the following relations:

$$\Delta G^{\#} = \Delta H^{\#} - T\Delta S^{\#}$$

and

$$\Delta H^{\#} = \mathrm{Ea} + \Delta \mathrm{ZPVE} + \Delta E(T)$$

RESULTS AND DISCUSSION

Kinetic and thermodynamic parameters

The gas phase eliminations of 2,2-diethoxy-ethylamine and 2,2-diethoxy-*N*,*N*-diethyl-ethylamine showed to occur through

Journal of Physical Organic Chemistry

Table 1. Kinetic and thermodynamic parameters of 2,2-diethoxy-ethylamine elimination at 340 °C

	Ea (kJ mol^{-1})	Log(A)	$\Delta S^{\neq}$ (J mol^{-1} K^{-1})	$\Delta H^{\neq}$ (kJ mol^{-1})	ΔG (kJ mol^{-1})
Step 1 Ethanol formation					
Experimental	201.1 ± 3.2	13.99 ± 0.27	8.60	196.0	190.2
MP2/6-31G	257.9	13.8	5.4	252.8	249.5
B3LYP/6-31G	**211.4**	**13.9**	**6.8**	**206.3**	**202.2**
B3LYP/6-31G(d,p)	224.4	13.4	−3.0	219.3	221.2
MPW91PW91/6-31G	233.3	14.4	15.7	228.2	218.6
MPW91PW91/6-31G(d,p)	239.4	13.5	−0.4	234.3	234.5
PBEPBE/6-31G	195.1	14.6	20.5	190.0	177.5
PBEPBE/6-31G(d,p)	**207.1**	**13.6**	**0.5**	**202.0**	**201.7**
Step 2 Ethane formation					
Experimental	203.8 ± 2.1	13.77 ± 0.18	4.39	198.7	196.0
MP2/6-31G	290.5	13.0	−10.0	285.4	291.6
B3LYP/6-31G	252.7	13.2	−7.2	247.6	252.0
B3LYP/6-31G(d,p)	277.7	13.5	−1.2	272.6	273.4
MPW91PW91/6-31G	267.6	13.1	−7.7	262.5	267.2
MPW91PW91/6-31G(d,p)	288.4	13.1	−7.6	283.3	288.0
PBEPBE/6-31G	**205.0**	**13.4**	**−3.5**	**199.9**	**202.0**
PBEPBE/6-31G(d,p)	239.1	13.7	3.7	234.0	231.7
Step 3 Ethylene formation					
Experimental	172.2 ± 1.0	11.88 ± 0.09	−31.79	167.1	186.6
MP2/6-31G	167.2	13.0	−10.3	162.1	168.4
MP2/6-31G(d,p)	174.3	12.7	−16.6	169.2	179.3
B3LYP/6-31G	161.5	13.3	−4.1	156.4	158.9
B3LYP/6-31G(d,p)	171.9	13.3	−4.2	166.8	169.4
MPW91PW91/6-31G	167.6	13.3	−5.0	162.5	165.5
MPW91PW91/6-31G(d,p)	**173.4**	**12.8**	**−13.7**	**168.3**	**176.7**
PBEPBE/6-31G	126.0	13.6	0.2	126.0	125.0

concerted parallel reactions. Thermodynamic and kinetic parameters are reported in Tables 1 and 2. The calculated parameters are in good agreement for PBEPBE method for ethanol and ethane formation from 2,2-diethoxy-ethylamine and 2,2-diethoxy-*N*,*N*-diethyl-ethylamine with the experimental values; however, for the consecutive reaction, step 3, MPW91PW91/6-31G (d,p) and MP2/6-31G (d,p) methods were found to be more adequate in describing this reaction (Tables 1 and 2).

In this work we found differences in DFT functional results, particularly ethanol and ethane formation from both substrates gave better parameters using PBEPBE while the consecutive step 3 render better values using MPW91PW91. These results suggest differences in the TS nature and correlation energy contributions for these processes. Activation energies are found to be similar for the parallel reactions, while step 3 exhibit lower activation energy. Considering the entropy of activation, both ethanol and ethane formation values are small positive compared to ethylene formation with entropy of activation about -30 kJ K^{-1} mol^{-1} for both substrates. These results imply a looser, polar TS structure for steps 1 and 2, and a more constrained TS structure for step 3.

Transition state and mechanism

The optimized TS structures for steps 1–3 are shown in Fig. 1 and Scheme 1. The TV associated to each imaginary frequency is shown in Fig. 1. Critical structures on the minimum energy path, MEP were characterized using vibrational analysis, and IRC calculations[8] were used to verify TS connecting reactants and products (Figs 2–7).

In the case of 2,2-diethoxy-ethylamine and 2,2-diethoxy-*N*,*N*-diethyl-ethylamine ethanol elimination (step 1) the reaction takes place through a four-membered transition state (TS1). Ethane formation from both substrates was also found to occur through four-membered TS (TS2). With respect to the consecutive reaction of ethylene formation, step 3, it was found to occur through a concerted, semi-polar six-membered cyclic transition state type of mechanism (TS3).

IRC calculations gave a configuration for the reactant that is higher in energy than the optimized reactant, suggesting that the substrate adopts a reactive-high energy conformation prior to the reaction for steps 1–3 from 2,2-diethoxy-ethylamine and 2,2-diethoxy-*N*,*N*-diethyl-ethylamine. Figures 2–7 show the reactants in the optimized conformation and the high energy conformation adopted to reach the TS, as well as the TS configuration.

Structural parameters are given in Tables 3–8, for steps 1–3 from both substrates. The TS for ethanol formation from of 2,2-diethoxy-ethylamine (step 1) is a quasi-planar geometry as shown in the small dihedrals (Table 3). Conversely, for 2,2-diethoxy-*N*,*N*-diethyl-ethylamine, the TS for ethanol formation is a four-membered structure shows small deviation

Table 2. Kinetic and thermodynamic parameters of 2,2-diethoxy-*N*,*N*-diethyl-ethylamine elimination at 340 °C

	Ea (kJ mol^{-1})	Log(A)	$\Delta S^{\neq}$ (J mol^{-1} K^{-1})	$\Delta H^{\neq}$ (kJ mol^{-1})	$\Delta G^{\neq}$ (kJ mol^{-1})
Step 1 Ethanol formation					
Experimental	202.3 ± 2.4	13.94 ± 0.20	7.64	197.2	192.6
B3LYP/6-31G	**205.7**	**14.1**	**10.2**	**200.6**	**194.3**
B3LYP/6-31G(d,p)	239.9	14.1	10.3	234.8	228.4
MPW91PW91/6-31G	229.4	13.6	1.0	224.3	223.7
MPW91PW91/6-31G(d,p)	253.7	14.3	13.9	248.6	240.1
PBEPBE/6-31G	190.0	14.5	17.4	184.9	174.2
PBEPBE/6-31G(d,p)	**208.8**	**14.8**	**24.4**	**203.7**	**188.8**
Step 2 Ethane formation					
Experimental	203.9 ± 2.6	14.03 ± 0.22	9.37	198.8	193.0
B3LYP/6-31G	241.3	11.2	−44.8	236.2	263.7
B3LYP/6-31G(d,p)	289.4	13.8	5.1	284.3	281.1
MPW91PW91/6-31G	275.1	13.1	−9.3	270.0	275.7
MPW91PW91/6-31G(d,p)	302.2	13.9	6.5	297.1	293.1
PBEPBE/6-31G	**208.4**	**13.9**	**6.6**	**203.3**	**199.3**
PBEPBE/6-31G(d,p)	226.6	13.7	3.1	221.5	219.6
Step 3 Ethylene formation					
Experimental	178.1 ± 2.3	12.02 ± 0.19	−29.11	173.0	190.8
MP2/6-31G	165.2	13.7	3.6	160.1	157.9
B3LYP/6-31G	174.1	12.8	−13.7	169.0	177.4
B3LYP/6-31G(d,p)	171.6	13.5	−0.8	166.5	167.1
MPW91PW91/6-31G	171.4	13.5	−1.7	166.3	167.4
MPW91PW91/6-31G(d,p)	**178.9**	**13.7**	**2.6**	**173.8**	**172.2**

from planarity (Table 6). Bond distances show intermediate progress for both molecules, however C—O distance appears more advanced, and the hydrogen being transferred is approximately equidistant to the carbon and oxygen atoms. For ethane formation the TS is a twisted four-membered cyclic structure for both molecules as seen in dihedrals (Tables 4 and 7). The TS show important C—O breaking in bond distances, and the hydrogen being transferred is located midway between the

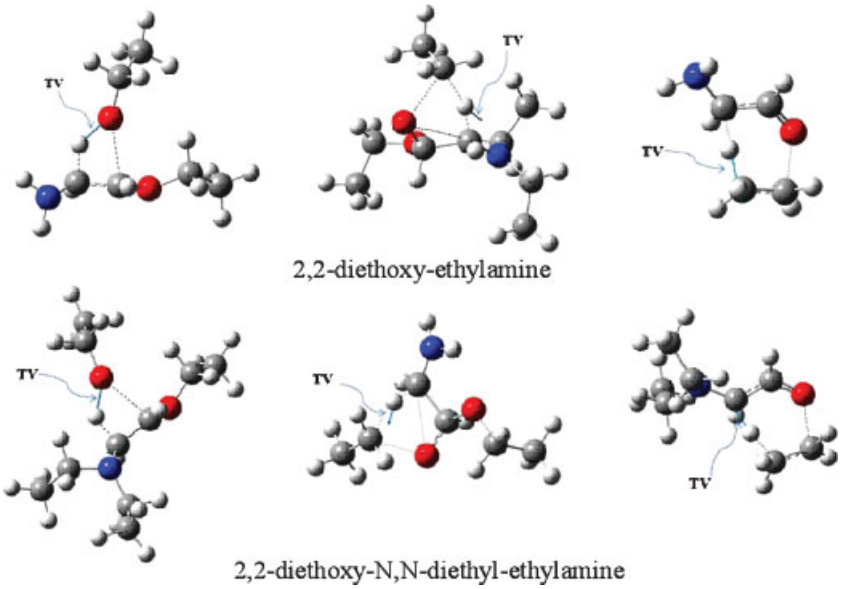

Figure 1. Optimized TS structures for 2,2-diethoxy-ethylamine (top) and 2,2-diethoxy-*N*,*N*-diethyl-ethylamine (bottom). TS for ethanol formation from 2,2-diethoxy-ethylamine (left-top) is quasi-planar four membered, while TS for ethanol formation from 2,2-diethoxy-*N*,*N*-diethyl-ethylamine show deviation from planarity (left-bottom). The TS leading to ethane formation (center-top, center bottom) are also four member structures, while TS for ethylene formation (right-top, right-bottom) TS are six-membered chair-like structures

Journal of Physical Organic Chemistry

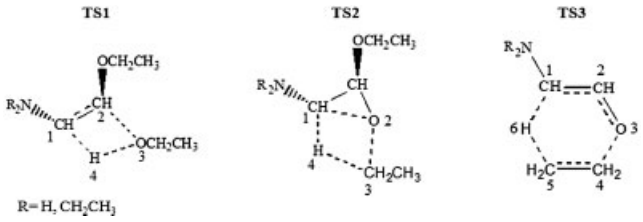

Scheme 1.

origin and final carbon atoms, however closer to the former. For the consecutive step 3 leading to ethylene formation the TS is a six-membered cyclic structure, in chair-like configuration with intermediate progress in bond distances (Tables 5 and 8).

Calculated NBO charges for ethanol, ethane, and ethylene formation steps 1–3 are given in Tables 9 and 10. For step 1, leading to ethanol formation there is an increase in negative charge in the oxygen atom and an increase in positive charge in the hydrogen atom being transferred for both compounds. The ethane formation step 2 shows more important changes in electron density in the oxygen atom, implying more polarization in the TS. For ethylene formation step 3, the changes in electron density observed in the TS include an increase in negative charge for C_1, an increase in positive charge for C_2, implying bond polarization for C_1—C_2, and small changes for the oxygen atom. In the TS, there is also an augmentation of negative charge in C_4.

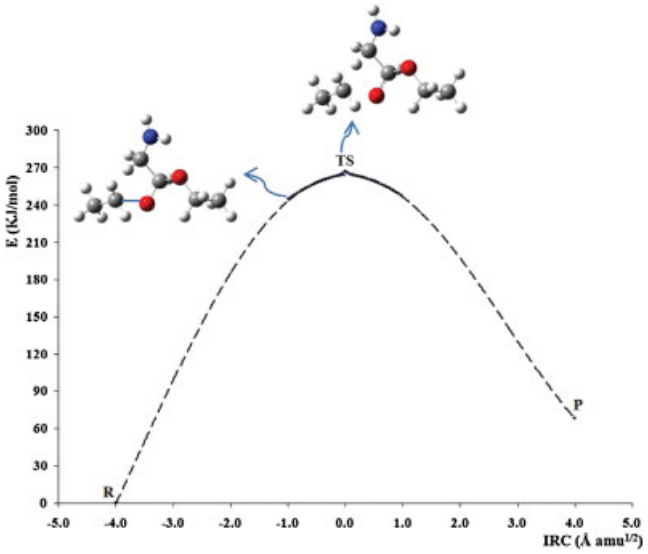

Figure 3. IRC reaction profile for 2,2-diethoxy-ethylamine thermal decomposition of step 2 at the B3LYP/6-31G level of theory

Bond order analysis

Reaction changes can better be described by NBO calculations estimating bond orders.[14–16] The Wiberg bond indexes[17] were calculated by means of the natural bond orbital NBO program[18] as implemented in Gaussian 03. A quantitative description of bond formation and bond breaking involved in the reaction mechanism can be monitored by means of the Synchronicity (Sy) concept proposed by Moyano *et al.*[19] defined by the expression

$$Sy = 1 - \frac{\left[\sum_{i=1}^{n} |\delta B_i - \delta B_{av}| / \delta B_{av}\right]}{(2n-2)}$$

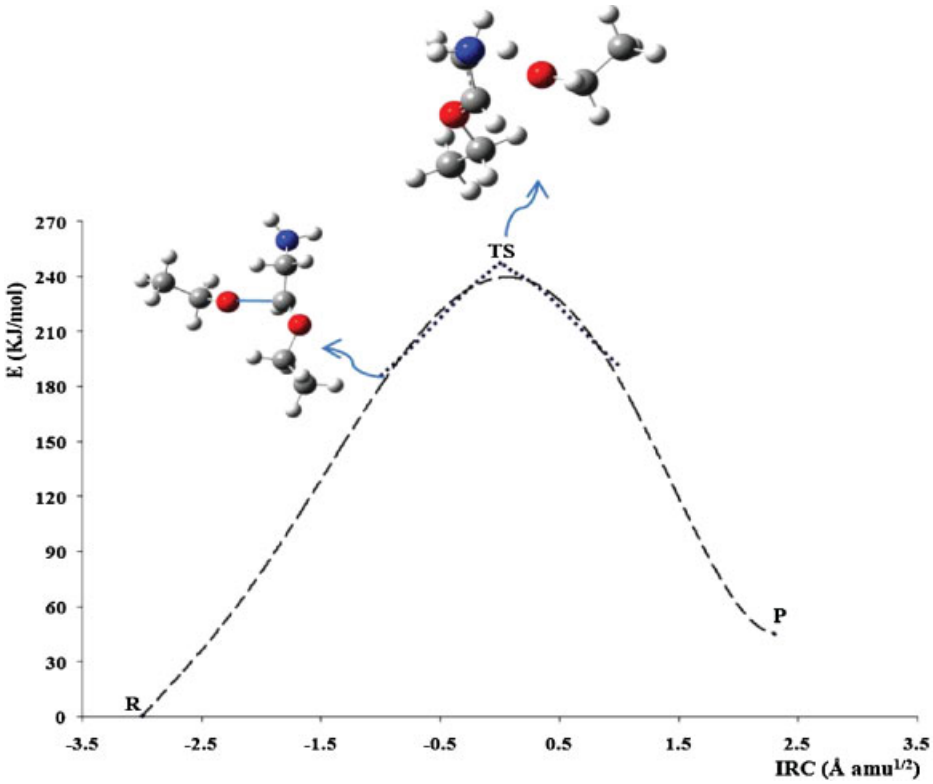

Figure 2. IRC reaction profile for 2,2-diethoxy-ethylamine thermal decomposition of step 1 at B3LYP/6-31G level of theory

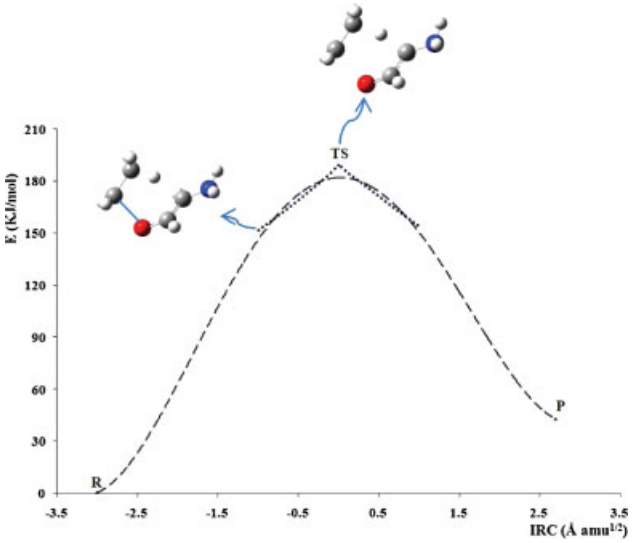

Figure 4. IRC reaction profile for 2,2-diethoxy-ethylamine thermal decomposition of step 3 at the B3LYP/6-31G level of theory

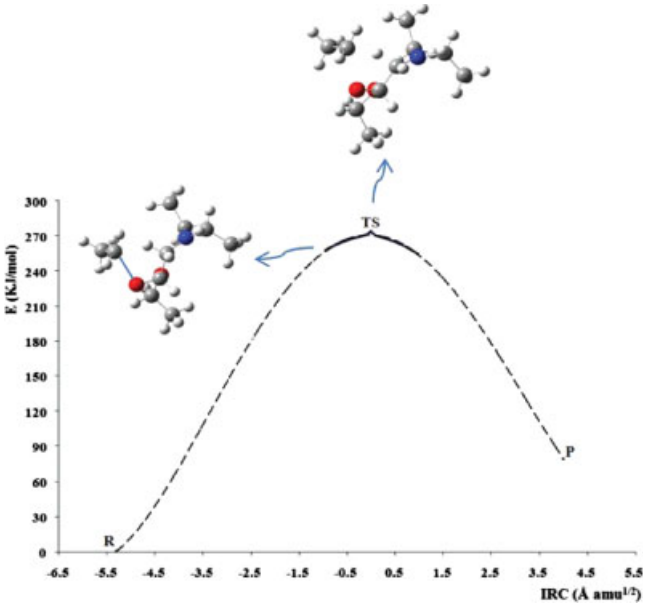

Figure 6. IRC reaction profile for 2,2-diethoxy-*N*,*N*-diethyl-ethylamine thermal decomposition of step 2 at the B3LYP/6-31G level of theory

n represents the number of bonds directly involved in the reaction and the relative variation of the bond index is obtained from

$$\delta B_i = \frac{[B_i^{TS} - B_i^{R}]}{[B_i^{P} - B_i^{R}]}$$

where the superscripts R, TS, P, represent reactant, transition state, and product, respectively. The evolution in bond change is calculated as

$$\%\text{Ev} = \delta B_i \times 100$$

The average value is calculated from

$$\delta B_{ave} = 1/n \sum_{i=1}^{n} \delta B_i$$

Bonds indexes were calculated for those bonds involved in the reaction changes, that is: for both cases in step 1 we used bonds C_1—C_2, C_2—O_3, O_3—H_4, and H_4—C_1; for step 2 C_1—O_2, O_2—C_3, C_3—H_4, H_4—C_1, and for step 3 bonds C_1—C_2, C_2—O_3, O_3—C_4, C_4—C_5, C_5—H_6, and H_6—C_1 were used. The remaining bonds remain practically unchanged and are not included in this analysis.

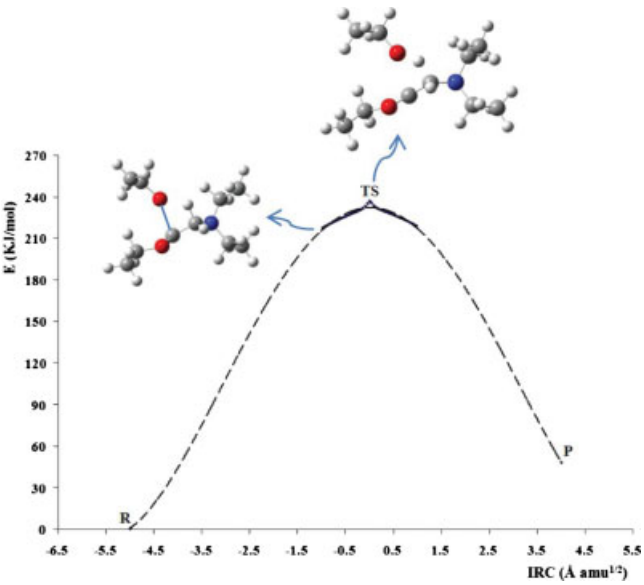

Figure 5. IRC reaction profile for 2,2-diethoxy-*N*,*N*-diethyl-ethylamine thermal decomposition of step 1 at the B3LYP/6-31G level of theory

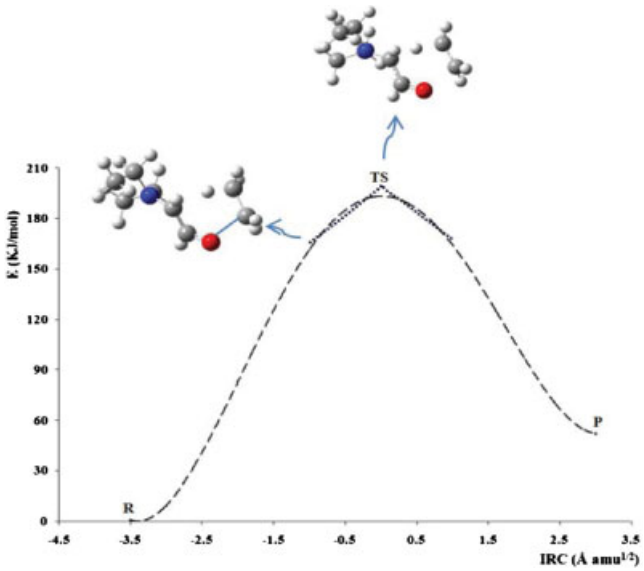

Figure 7. IRC reaction profile for 2,2-diethoxy-*N*,*N*-diethyl-ethylamine thermal decomposition of step 3 at the B3LYP/6-31G level of theory

Journal of Physical Organic Chemistry

Table 3. Structural parameters for 2,2-diethoxy-ethylamine (R), four-membered ring transition state (TS), and products (P) for step 1 at PBEPBE/6-31G(d,p) level

	Atom distances (Å)			
	C_1–C_2	C_2–O_3	O_3–H_4	H_4–C_1
R	1.537	1.406	2.571	1.104
TS	1.436	2.135	1.384	1.311
P	1.354	3.214	0.982	2.418
	Dihedral angles (degrees)			
	C_1–C_2–O_3–H_4	C_2–O_3–H_4–C_1	O_3–H_4–C_1–C_2	H_4–C_1–C_2–O_3
TS	−1.443	2.346	−2.916	1.272
	Imaginary frequency (cm^{-1})			
TS	1529.6			

Table 4. Structural parameters for 2,2-diethoxy-ethylamine (R), four-membered ring transition state (TS), and products (P) for step 2 at PBEPBE/6-31G level

	Atom distances (Å)			
	C_1–O_2	O_2–C_3	C_3–H_4	H_4–C_1
R	2.467	1.474	3.759	1.104
TS	2.400	2.250	1.582	1.208
P	1.670	4.287	1.106	4.198
	Dihedral angles (degrees)			
	C_1–O_2–C_3–H_4	O_2–C_3–H_4–C_1	C_3–H_4–C_1–O_2	H_4–C_1–O_2–C_3
TS	−4.618	21.900	−20.820	6.150
	Imaginary frequency (cm^{-1})			
TS	521.8			

Table 5. Structural parameters for 2-ethoxy-ethenamine (R), six-membered ring transition state (TS), and products (P) for step 3 at MPW91PW91/6-31G(d,p) level

	Atom distances (Å)					
	C_1–C_2	C_2–O_3	O_3–C_4	C_4–C_5	C_5–H_6	H_6–C_1
R	1.345	1.373	1.429	1.518	1.087	2.790
TS	1.413	1.272	2.073	1.401	1.317	1.457
P	1.519	1.223	3.512	1.337	2.988	1.090
	Dihedral angles (degrees)					
	C_1–C_2–O_3–C_4	C_2–O_3–C_4–C_5	O_3–C_4–C_5–H_6	C_4–C_5–H_6–C_1	C_5–H_6–C_1–C_2	H_6–C_1–C_2–O_3
TS	−65.989	28.442	−4.931	31.740	−57.785	60.810
	Imaginary frequency (cm^{-1})					
TS	955.9					

Table 6. Structural parameters for 2,2-diethoxy-*N*,*N*-diethyl-ethylamine (R), four-membered ring transition state (TS), and products (P) for step 1 at PBEPBE/6-31G(d,p) level

	Atom distances (Å)			
	C_1–C_2	C_2–O_3	O_3–H_4	H_4–C_1
R	1.532	1.460	2.700	1.100
TS	1.437	2.240	1.410	1.250
P	1.357	3.410	0.980	4.430
	Dihedral angles (degrees)			
	C_1–C_2–O_3–H_4	C_2–O_3–H_4–C_1	O_3–H_4–C_1–C_2	H_4–C_1–C_2–O_3
TS	−6.786	10.270	−13.580	6.500
	Imaginary frequency (cm^{-1})			
TS		631.7		

Table 7. Structural parameters for 2,2-diethoxy-*N*,*N*-diethyl-ethylamine (R), four-membered ring transition state (TS), and products (P) for step 2 at PBEPBE/6-31G level

	Atom distances (Å)			
	C_1–O_2	O_2–C_3	C_3–H_4	H_4–C_1
R	2.451	1.430	4.230	1.100
TS	2.358	2.250	1.610	1.190
P	1.530	3.560	1.100	3.060
	Dihedral angles (degrees)			
	C_1–O_2–C_3–H_4	O_2–C_3–H_4–C_1	C_3–H_4–C_1–O_2	H_4–C_1–O_2–C_3
TS	6.670	−27.060	25.680	−8.960
	Imaginary frequency (cm^{-1})			
TS		470.6		

Table 8. Structural parameters of 2-ethoxy-*N*,*N*-diethyl-ethenamine (R), six-membered ring transition state (TS), and products (P) for step 3 at MPW91PW91/6-31G(d,p) level

	Atom distances (Å)					
	C_1–C_2	C_2–O_3	O_3–C_4	C_4–C_5	C_5–H_6	H_6–C_1
R	1.343	1.360	1.410	1.520	1.090	2.810
TS	1.415	1.250	2.110	1.390	1.330	1.470
P	1.513	1.200	3.530	1.320	6.290	1.090
	Dihedral angles (degrees)					
	C_1–C_2–O_3–C_4	C_2–O_3–C_4–C_5	O_3–C_4–C_5–H_6	C_4–C_5–H_6–C_1	C_5–H_6–C_1–C_2	H_6–C_1–C_2–O_3
TS	−64.830	28.410	−3.800	26.060	−48.640	58.370
	Imaginary frequency (cm^{-1})					
TS			1046.3			

Table 9. NBO charges of the atoms for the R, TS, and P in the elimination reaction of 2,2-diethoxy-ethylamine

Step 1 Ethanol formation (PBEPBE/6-31G(d,p))				Step 2 Ethane formation (PBEPBE/6-31G)				Step 3 Ethylene formation (MPW91PW91/6-31G(d,p))			
	R	TS	P		R	TS	P		R	TS	P
C_1	−0.133	−0.298	−0.024	C_1	−0.178	−0.117	0.132	C_1	−0.166	−0.254	−0.402
C_2	0.334	0.291	0.104	O_2	−0.450	−0.451	−0.442	C_2	0.043	0.239	0.399
O_3	−0.438	−0.539	−0.512	C_3	−0.092	−0.281	−0.463	O_3	−0.538	−0.576	−0.535
H_4	0.115	0.275	0.311	H_4	0.184	0.158	0.134	C_4	−0.130	−0.308	−0.455
								C_5	−0.746	−0.721	−0.460
								H_6	0.245	0.266	0.273

Bond orders from NBO calculations for elimination steps 1–3 for both compounds are given in Tables 11 and 12. For steps 1 and 2, the most advanced reaction coordinate is the breaking of C—O bond in the order of 57–61% evolution. In the case of ethanol forming step 1, the second most advanced reaction coordinate is the breaking of bond C—H corresponding to the hydrogen being transferred. For ethane formation step 2 all coordinates other than C—O breaking are less advanced in the TS (24–29% evolution). In the case of step 3, the bonds involving the oxygen atom (C_2—O_3 and O_3—C_4), and the change of C_1—C_2 bond order from single to double bond, show the greatest progress in the reaction coordinate (56–66% evolution), and O_3—C_4 bond breaking is the limiting factor. The remaining coordinates are earlier in the TS configuration (40–42%).

The synchronicity parameters Sy = 0.76–0.78 for ethane formation suggest a polar asynchronic mechanism for both substrates, while ethanol and ethylene formation, steps 1 and 3, are more synchronous implying a less polarized TS and exhibit Sy values ranging from 0.86 to 0.91.

Calculations show that the least polar asynchronic process, step 3, leading to ethylene formation, is better described using DFT functional MPW91PW91. However, good results for steps 1 and 2 were obtained by DFT functional PBEPBE. The PBE functional is a derivation of GGA with construction underlying PW91 GGA functional.[20] PBEPBE is improved over PW91 and retains some features of LSD and combines them with the more energetically favored features of gradient-corrected non-locality. It is interesting that PBEPBE functional appears to be inadequate to describe the ethylene formation (step 3) while giving reasonably good calculated parameters for steps 1 and 2. These results suggest that the TS for ethanol (step 1) and ethane formation (step 2) different contributions of the local and non-local varying density in the TS compared to ethylene formation.

The mechanism for ethane formation has been recently reported,[6] where it was proposed that $O^{\delta-}$ is stabilized toward the Cα to form the carbonyl, while the H atom migrates to the Cγ to form the corresponding ethyl ester of the amino acid and ethane gas [reaction (3)]. This mechanistic consideration is discarded because of the high energy of activation for the transition state formation (>300 kJ mol^{-1}). In this respect, the present work shows that the TS for this reaction (step 2) is a four-membered cycle and more polar in nature than the TS leading to ethanol formation. In step 2, there is a significant advance in the C—O bond breaking compared to all other reaction coordinates, while in step 1 the transfer of the hydrogen

Table 10. NBO charges of the atoms for the R, TS, and P in the elimination reaction of 2,2-diethoxy-*N*,*N*-diethyl-ethylamine

Step 1 Ethanol formation (PBEPBE/6-31G(d,p))				Step 2 Ethane formation (PBEPBE/6-31G)				Step 3 Ethylene formation (MPW91PW91/6-31G(d,p))			
	R	TS	P		R	TS	P		R	TS	P
C_1	−0.327	−0.409	−0.112	C_1	−0.335	−0.248	0.090	C_1	−0.153	−0.255	−0.393
C_2	0.374	0.302	0.031	O_2	−0.586	−0.600	−0.640	C_2	0.023	0.251	0.401
O_3	−0.560	−0.745	−0.749	C_3	−0.167	−0.442	−0.741	O_3	−0.542	−0.576	−0.546
H_4	0.241	0.389	0.475	H_4	0.255	0.250	0.270	C_4	−0.129	−0.308	−0.451
								C_5	−0.747	−0.719	−0.458
								H_6	0.247	0.266	0.267

Table 11. NBO analysis for 2,2-diethoxy-ethylamine elimination. Wiberg bond indexes (B_i), % evolution through the reaction coordinate (%Ev), are shown for reactants R, TS, and products P. Average bond index variation (δB_{av}) and synchronicity parameter (Sy)

Step 1 Ethanol formation (PBEPBE/6-31G(d,p))							
	C_1–C_2	C_2–O_3	O_3–H_4	H_4–C_1			Sy
B_i^R	0.9744	0.8897	0.0013	0.9049			
B_i^{ET}	1.2244	0.3547	0.2811	0.4782			0.861
B_i^P	1.7512	0.0081	0.7194	0.0134			
%Ev	32.18	60.69	38.96	47.86			
Step 2 Ethane formation (PBEPBE/6-31G)							
	C_1–O_2	O_2–C_3	C_3–H_4	H_4–C_1			
B_i^R	0.0277	0.9011	0.0002	0.8873			
B_i^{ET}	0.1858	0.3780	0.2705	0.6271			0.782
B_i^P	0.6907	0.0004	0.9289	0.0000			
%Ev	23.85	58.08	29.11	29.33			
Step 3 Ethylene formation (MPW91PW91/6-31G(d,p))							
	C_1–C_2	C_2–O_3	O_3–C_4	C_4–C_5	C_5–H_6	H_6–C_1	
B_i^R	1.7915	0.9968	0.8973	1.0259	0.9218	0.0010	
B_i^{ET}	1.3068	1.4888	0.3044	1.4578	0.4755	0.3555	0.901
B_i^P	0.9891	1.8645	0.0043	2.0360	0.0018	0.8808	
%Ev	60.41	56.70	66.39	42.76	48.51	40.29	

Table 12. NBO analysis for 2,2-diethoxy-*N*,*N*-diethyl-ethylamine elimination. Wiberg bond indexes (B_i), % evolution through the reaction coordinate (%Ev), are shown for reactants R, TS, and products P. Average bond index variation (δB_{av}) and synchronicity parameter (Sy)

Step 1 Ethanol formation (PBEPBE/6-31G(d,p))							
	C_1–C_2	C_2–O_3	O_3–H_4	H_4–C_1			Sy
B_i^R	0.9803	0.8885	0.0020	0.8978			
B_i^{ET}	1.2237	0.3516	0.2536	0.5345			0.910
B_i^P	1.7422	0.0002	0.7574	0.0000			
%Ev	31.95	60.44	33.31	40.47			
Step 2 Ethane formation (PBEPBE/6-31G)							
	C_1–O_2	O_2–C_3	C_3–H_4	H_4–C_1			
B_i^R	0.0240	0.882	0.0004	0.8996			
B_i^{ET}	0.1237	0.3726	0.2451	0.6523			0.764
B_i^P	0.4498	0.0096	0.8908	0.0003			
%Ev	23.42	58.39	27.48	27.50			
Step 3 Ethylene formation (MPW91PW91/6-31G(d,p))							
	C_1–C_2	C_2–O_3	O_3–C_4	C_4–C_5	C_5–H_6	H_6–C_1	
B_i^R	1.7581	0.9854	0.9017	1.0248	0.9205	0.0011	
B_i^{ET}	1.2981	1.492	0.304	1.451	0.4796	0.3543	0.894
B_i^P	0.9985	1.8477	0.0024	2.0379	0	0.8795	
%Ev	60.56	58.75	66.46	42.07	47.90	40.21	

Journal of Physical Organic Chemistry

is also important. The proposed mechanism for ethanol, ethane, and ethylene formation for 2,2-diethoxy-ethylamine and 2,2-diethoxy-*N*,*N*-diethyl-ethylamine is illustrated in reaction (4).

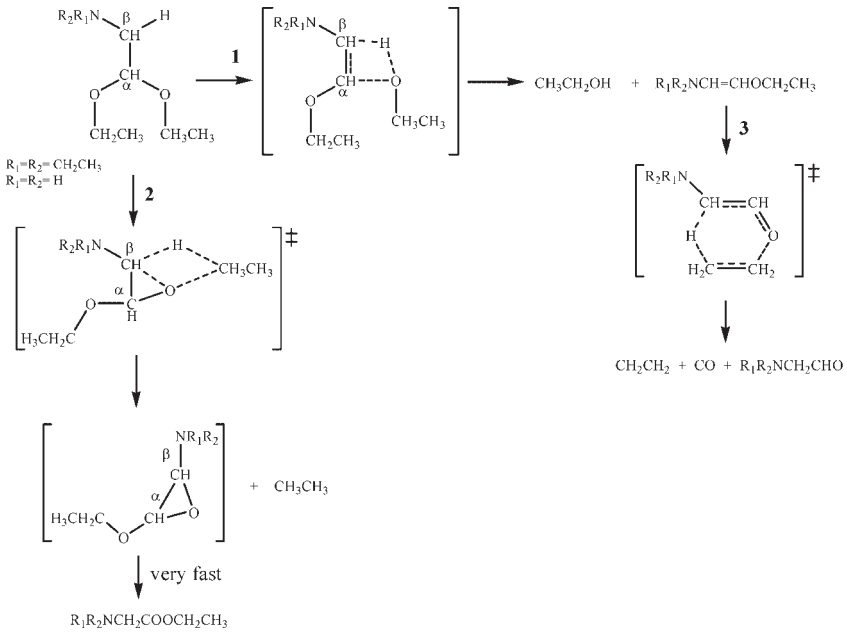

(4)

CONCLUSIONS

In this work, we studied the thermal elimination reaction from 2,2-diethoxy-ethylamine and 2,2-diethoxy-*N*,*N*-diethyl-ethylamine which occurs forming different products in a complex reaction scheme involving parallel and consecutive reactions.[6] The reaction leading to ethanol formation, step 1 takes place through four-membered cyclic TS moderately polar asynchronic. The parallel reaction forming ethane, step 2, Sy = 0.76–0.78, is more polar, less synchronic than ethanol formation. In parallel reactions steps 1 and 2, the rate-determining process is the breaking of C—O bond, however in ethanol formation the hydrogen transfer is also important. The consecutive reactions leading to ethylene formation occur in a semi-polar asynchronic type of mechanism with chair-like six-membered cyclic TS structure. Calculations show good agreement to experimental values using PBEPBE functional to describe steps 1 and 2, while step 3 is better described using MPW91PW91 suggesting difference in electron density variations in these reactions.

REFERENCES

[1] M. Molera, J. Centeno, J. Orza, *J. Chem. Soc.* **1963**, 2234–2241.
[2] M. Molera, J. Fernandez-Biarge, J. Centeno, L. Arévalo, *J. Chem. Soc.* **1963**, 2311–2320.
[3] M. Molera, G. Dominguez, *Anal. Real. Soc. Esp. Fis. y Quim.* **1963**, *11*, 639–648.
[4] M. Molera, G. Pereira, *Anal. Fis. Quim.* **1966**, *62*, 661–666.
[5] M. Molera, G. Pereira, *Anal. Fis. Quim.* **1966**, *62*, 667–675.
[6] J. R. Mora, R. M. Domínguez, A. Herize, M. Tosta, G. Chuchani, *J. Phys. Org. Chem.* **2008**, *21*, 359–364.
[7] Gaussian 03, Revision B.01, M. J. Frisch, G. W. Trucks, H. B. Schlegel, G. E. Scuseria, M. A. Robb, J. R. Cheeseman, J. A. Montgomery, Jr., T. Vreven, K. N. Kudin, J. C. Burant, J. M. Millam, S. S. Iyengar, J. Tomasi, V. Barone, B. Mennucci, M. Cossi, G. Scalmani, N. Rega, G. A. Petersson, H. Nakatsuji, M. Hada, M. Ehara, K. Toyota, R. Fukuda, J. Hasegawa, M. Ishida, T. Nakajima, Y. Honda, O. Kitao, H. Nakai, M. Klene, X. Li, J. E. Knox, H. P. Hratchian, J. B. Cross, C. Adamo, J. Jaramillo, R. Gomperts, R. E. Stratmann, O. Yazyev, A. J. Austin, R. Cammi, C. Pomelli, J. W. Ochterski, P. Y. Ayala, K. Morokuma, G. A. Voth, P. Salvador, J. J. Dannenberg, V. G. Zakrzewski, S. Dapprich, A. D. Daniels, M. C. Strain, O. Farkas, D. K. Malick, A. D. Rabuck, K. Raghavachari, J. B. Foresman, J. V. Ortiz, Q. Cui, A. G. Baboul, S. Clifford, J. Cioslowski, B. B. Stefanov, G. Liu, A. Liashenko, P. Piskorz, I. Komaromi, R. L. Martin, D. J. Fox, T. Keith, M. A. Al-Laham, C. Y. Peng, A. Nanayakkara, M. Challacombe, P. M. W. Gill, B. Johnson, W. Chen, M. W. Wong, C. Gonzalez, J. A. Pople, Gaussian, Inc., Pittsburgh PA, **2003**.
[8] A. Deborah, E. José, *J. Chem. Educ.* **2006**, *83*, 69–76.
[9] D. McQuarrie, *Statistical Mechanics*, Harper & Row, New York, **1986**.
[10] J. B. Foresman, Æ. Frish, *Exploring Chemistry With Electronic Methods* (2nd edn), Gaussian, Inc., Pittsburgh, PA, **1996**.
[11] S. W. Benson, *The Foundations of Chemical Kinetics*, McGraw-Hill, New York, **1960**.
[12] H. E. O'Neal, S. W. Benson, *J. Phys. Chem.* **1967**, *71*, 2903–2921.
[13] S. W. Benson, *Thermochemical Kinetics*, John Wiley & Sons, New York, **1968**.
[14] G. J. Lendvay, *J. Phys. Chem.* **1989**, *93*, 4422–4429.
[15] A. E. Reed, R. B. Weinstock, F. Weinhold, *J. Chem. Phys.* **1985**, *83*(2), 735–746.
[16] A. E. Reed, L. A. Curtiss, F. Weinhold, *Chem. Rev.* **1988**, *88*, 899–926.
[17] K. B. Wiberg, *Tetrahedron*, **1968**, *24*, 1083–1095.
[18] E. D. Glendening, A. E. Reed, J. E. Carpenter, F. Weinhold, NBO version 3.1.
[19] A. Moyano, M. A. Periclas, E. Valenti, *J. Org. Chem.* **1989**, *54*, 573–582.
[20] J. P. Perdew, K. Burke, M. Ernserhof, *Phys. Rev. Lett* **1996**, *77*(8), 3865–3868.